24SNVH-0048

Using the irrotational intensity field to study vibration energy paths in automotive structures

xxxxxxxxx
xxxxxxx, xxxxxxxxx

ABSTRACT

Although structural intensity was introduced in the 80's, this concept never found practical applications, neither for numerical nor experimental approaches. Quickly, it has been pointed out that only the irrotational component of the intensity offers an easy interpretation of the dynamic behavior of structures by visualizing the vibration energy flow. This is especially valuable at mid and high frequency where the structure response understanding can be challenging. A new methodology is proposed in order to extract this irrotational intensity field from the Finite Element Model of assembled structures such as Bodies In White. This methodology is hybrid in the sense that it employs two distinct solvers: a dynamic solver to compute the structural dynamic response and a thermal solver to address a diffusion equation analogous to the thermal conduction built from the previous dynamic response. The field separation is based on the Helmholtz-Hodge theorem, which ensures the computation's full consistency. The methodology is first implemented and validated in the case of a plate assembly, using commercial FE software. This first approach immediately highlights a bias in the current power flow computations, leading to erroneous transmission path understanding. It also shows a remarkable stability of the irrotational intensity patterns regarding frequency. As one would expect, transmission path only makes sense when they stand for a broad enough frequency range. The methodology is then applied to an automotive structure, introducing specific modeling of the mechanical connections between stamped steel parts (spot welds, bolts, bids...). Again the method applies well and shows fully consistent results.

INTRODUCTION

Introduced around the 1980s ([1], [2]), the structural intensity concept never found wide practical applications, neither for numerical nor experimental approaches. Quickly, it has been pointed out that only the irrotational component of the intensity offers an easy interpretation of the dynamic behavior of structures by visualizing the vibration energy flow (See [3]). Such an approach would be especially valuable at mid and high frequencies where structure-borne noise is predominant. Indeed, the high modal density prevents the use of standard low frequency analyses based on modal shapes or operational deflections.

Most mid-high frequencies approaches developed since the 1960s rely on energy concepts such as power flow and acoustic or vibrational temperature ([4], [5]). Statistical Energy Analysis (SEA) nevertheless assumes that power flows between subsystems are proportional to the difference of modal energies (eg vibrational temperature). The method was widely used for large structures such as ships, buildings, or rockets for which substructures identification is rather straightforward since they mostly consist in shells, plates, and beams assemblies ([6]). Continuous power flow approaches were later developed for plates and beams in order to achieve more local predictions ([7], [8]). Most of these approaches deal with homogenous structures for which wave propagation remains a useful tool.

Automobile structures, on the contrary, are highly heterogeneous and complex in their assembly. The Final Element Method then appears as the only relevant tool to model the structural stiffness resulting from curvature and corrugations. Attempts to use SEA ([9]) or energy methods ([10]) for vehicle structures collide with the method's

intrinsic assumptions, requiring a high level of expertise for a proper application.

Therefore, a new methodology ([11]) was proposed in order to compute the full energy flow scheme (namely the irrotational intensity field) and vibrational temperature from the Finite Element Model of assembled structures such as vehicle Bodies In White (BIW). This methodology is hybrid in the sense that it employs two distinct solvers: a dynamic solver to compute the structural dynamic response and a thermal solver to address a diffusion equation analogous to the thermal conduction built from the previous dynamic response and providing the expected energetical quantities. This paper deals with the extension of the method to the case of assembled structures, involving incompatible meshes and mechanical connections.

After setting the method theoretical foundation, it is first implemented and validated in the case of a plate assembly, using commercial FE software. It is then applied to an automotive structure, introducing specific modeling of the mechanical connections between stamped steel parts (spot welds, bolts, bids...).

ENERGETICAL QUANTITIES DEFINITIONS

The instantaneous structural intensity, a time-dependent vector, represents the variation in energy density within a minuscule volume in a structure. It is mathematically defined at a point M of the structure and at time t as

$$\mathbf{I}(M,t) = -\boldsymbol{\sigma}(M,t)\mathbf{v}(M,t). \tag{1}$$

Here, $\boldsymbol{\sigma}(M,t)$ and $\mathbf{v}(M,t)$ refer to the stress tensor and velocity vector, respectively.

For steady-state harmonic vibrations at a given frequency ω, the time-averaged structural intensity over a period represents the net energy flow. This average can be expressed as

$$\mathbf{I}(M,\omega) = -\frac{1}{2}\Re(\boldsymbol{\sigma}(M,\omega)\mathbf{v}^*(M,\omega)), \tag{2}$$

where $\boldsymbol{\sigma}(M,\omega)$ and $\mathbf{v}(M,\omega)$ signify the stress tensor and velocity vector at point M respectively, and $\Re$ stands for the real part of a complex number. The symbol * denotes the complex conjugate operator. For brevity, M and ω are later omitted.

The injected input power into the structure through a single point is expressed as

$$P_{inj} = \frac{1}{2}\Re(\mathbf{F}.\mathbf{v}_{in}^*), \tag{3}$$

where $\mathbf{F}$ is the excitation force vector applied to the structure, and $\mathbf{v_{in}}$ is the velocity vector at the excitation point. Results are typically normalized to a unit input power due to the proportional nature of energy quantities.

When the dissipation is due to structural (hysteretic) damping, the power dissipated per unit area within a structure vibrating in the harmonic regime at frequency ω is typically formulated as [12]

$$P_{diss} = 2\eta\omega E_d, \tag{4}$$

where η denotes the implicitly frequency-dependent structural damping loss factor and E_d stands for the strain energy density. Without loss of generality, only structural damping is considered in the following.

The local energy balance in steady-state harmonic vibrations of an elastic medium is expressed using the divergence of the structural intensity field [12]

$$\boldsymbol{\nabla}.\mathbf{I} = P_{inj} - P_{diss}, \tag{5}$$

where $\boldsymbol{\nabla}.$ is the divergence operator.

The structural intensity divergence can thus be estimated through the injected power and the dissipated power per unit area within the structure.

The power flow through a cross-section S is computed using

$$P_f = \iint_S \mathbf{I}.\mathbf{ds} \tag{6}$$

For structures assemblies, the power flow from substructure i to substructure j is expressed in terms of structural intensity by the formula

$$P_{i\to j} = \iint_{S_b} \mathbf{I}.\mathbf{ds}\ . \tag{7}$$

Here, S_b denotes the common section shared by substructures i and j.

IRROTATIONAL INTENSITY FIELD COMPUTATION

By applying the Hodge Helmholtz decomposition, as introduced in [13], the structural intensity field $\mathbf{I}$ can be separated into three components: $\mathbf{I}_r$ the rotational intensity, an irrotational intensity $\mathbf{I}_{ir}$, and a harmonic part $\mathbf{h}$ such that

$$\mathbf{I} = \mathbf{I}_r + \mathbf{I}_{ir} + \mathbf{h}. \tag{8}$$

The irrotational intensity is derived from a scalar potential ψ as

$$\mathbf{I}_{ir} = -\boldsymbol{\nabla}\psi. \tag{9}$$

$\boldsymbol{\nabla}$ stands here for the gradient operator and $\mathbf{I}_{ir}$ characterizes the energy transfer from injected power sources to dissipative regions, as discussed in [3].

Through the application of the Helmholtz-Hodge decomposition, the local power balance is reformulated as

$$\begin{aligned}\boldsymbol{\nabla}.\mathbf{I} &= \boldsymbol{\nabla}.(\mathbf{I}_r + \mathbf{I}_{ir} + \mathbf{h}) \\ &= \boldsymbol{\nabla}.(\boldsymbol{\nabla} \wedge \mathbf{A}) + \boldsymbol{\nabla}.(-\boldsymbol{\nabla}\psi) + \boldsymbol{\nabla}.\mathbf{h}.\end{aligned}$$

The divergence of both the rotational intensity and the harmonic component being null, one gets

$$\boldsymbol{\nabla}.\mathbf{I} = -\boldsymbol{\nabla}.\boldsymbol{\nabla}\psi. \tag{10}$$

It is noteworthy that the total structural intensity and the irrotationnal intensity share the same divergence, $\boldsymbol{\nabla}.\boldsymbol{\nabla}\psi$, that is to say the same local energy balance. As a consequence, the power flow crossing any closed contour inside the structure only depends on the irrotational component. Thus, the propagation of vibration energy can exclusively be described in terms of the irrotational intensity.

Due to its rotational nature, the rotational intensity cannot originate or terminate at an energy source or sink; instead, it forms closed loops or extends infinitely. This rotational characteristic does not influence the quantitative assessment of vibration energy transfer through any closed contour. The nature, origin and properties of the rotational intensity field will not be discussed here.

By combining the local energy balance in steady-state Eq.(5) and Eq.(10), a novel equation governing the flow of vibration energy is derived. The equation is similar to the heat conduction equation

$$-\boldsymbol{\nabla}.\boldsymbol{\nabla}\psi = P_{inj} - P_{diss}. \tag{11}$$

Eq. (11) underscores the direct correlation between the irrotational intensity and energy sources and sinks. To obtain this vector field, the solution to Eq. (11) is required, where the potential scalar ψ is the unknown quantity, and its gradient $\boldsymbol{\nabla}\psi$ signifies the irrotational intensity field. The right-hand side of the equation is derived from the dynamic response under harmonic excitation. The dissipated power is calculated using Eq. (4), while the injected power is determined by Eq. (3). From a practical standpoint, the injected power can be treated as a thermal source in the diffusion equation in the diffusion Eq.(11), which can then be solved with a thermal solver.

BOUNDARY CONDITIONS

To solve Eq. (11) within the specified domain, boundary conditions are essential. In the context of a structural problem where there is no energy transfer beyond the structure and no dissipation at the system's boundary, energy-free boundaries will be considered. This assumption implies that the normal energy flow is zero at these free boundaries, indicating a complete reflection of the energy flow. The boundary conditions can then be expressed as follows:

$$\boldsymbol{\nabla}\psi.\mathbf{n} = \frac{\partial\psi}{\partial n} = 0, \tag{12}$$

where **n** is the unit vector normal to the considered boundary.

This boundary condition is the natural boundary condition of the thermal finite element model on free edges.

POWER FLOW DECOMPOSITION

Similar to the structural intensity field, the power flow through a cross-section S can be decomposed into two components: irrotational power flow P_{ir} and rotational power flow P_r. The total power flow represented by the structural intensity can then be rewritten as follows:

$$P_f = P_{ir} + P_r, \tag{13}$$

where

$$P_{ir} = \iint_S \mathbf{I_{ir}}.\mathbf{ds} \tag{14}$$

$$P_r = \iint_S \mathbf{I_r}.\mathbf{ds}\ . \tag{15}$$

This will allow further computations of the power flow exchanges within the studied structure. Again, it is to be noticed that the power flow associated with the rotationnal intensity is null for exchanges through closed contours.

IRROTATIONAL INTENSITY IN ASSEMBLED STRUCTURES

The proposed method for determining irrotational intensity in assembled structures involves solving the diffusion equation, with the application of boundary conditions that enforce zero flux along the edges. Connections between the model components are considered within the thermal analysis framework, utilizing specific thermal models. These models aim to represent the continuity of the energy fields. To illustrate this concept, Fig. 1 provides an example of a connection model. In this schematic, two sub-structures, labeled as 1 and 2, are joined using connection elements such as RBE2, RBE3, MPC, eventually in combination with undamped elements such as CBAR, CBUSH, CELAS...

For such non-dissipative connections, the energy entering the system at point A equals the energy leaving at point B, with no energy loss and a continuity of the vibrational temperature.

Complex connections (joints, glue) may include dissipations. In this case, specific elements (CBAR, CBUSH,

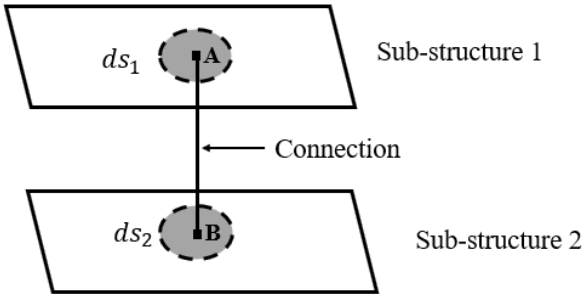

Fig. 1. Connection model

CHEXA,...) are used to provide the dissipation. Dissipating elements should then be considered as a substructure connected on both sides by non-dissipative connections.

The mathematical formulation of power exchange between two substructures at points A and B can be expressed using the irrotational intensity as follows:

$$P_A = \lim_{ds_1 \to 0} \iint \boldsymbol{\nabla}\psi.\mathbf{ds}, \tag{16}$$

$$P_B = \lim_{ds_2 \to 0} \iint \boldsymbol{\nabla}\psi.\mathbf{ds}. \tag{17}$$

In the case of a non-dissipative connection, when the surface elements ds_1 et ds_2 tend to zero, the flux conservation leads to

$$\boldsymbol{\nabla}\psi_A = \boldsymbol{\nabla}\psi_B. \tag{18}$$

This indicates that the continuity of vibratory energy flow, as represented by irrotational intensity, is maintained across the connection that links the two systems. In simpler terms, vibration energy is transferred from one side of the interface to the other without any loss. Given that the potential ψ is continuously differentiable across the entire structure, including the connection zone, this implies:

$$\psi_A = \psi_B. \tag{19}$$

The vibrational temperature appears to be the same on both sides of a non-dissipative connection. This condition is incorporated into the thermal finite element model by introducing linear relationships (MPC) among nodes associated with a non-dissipative connection. These linear relationships ensure the equality of vibrational temperature across all corresponding nodes in a mean square sense.

Therefore, the problem to be solved is formulated as follows:

$$\begin{cases} -\boldsymbol{\nabla}.\boldsymbol{\nabla}\psi = P_{inj} - P_{diss} \\ \boldsymbol{\nabla}\boldsymbol{\psi}.\mathbf{n} = 0 \text{ sur } \partial\Omega \\ \psi_A = \psi_B \end{cases} \tag{20}$$

NUMERICAL IMPLEMENTATION

Firstly, a structural dynamic response under harmonic excitation is performed, in order to compute the right-hand side of Eq.(11). The dissipated power per unit area P_{diss} is derived from the strain energy density, while the injected power P_{inj} is evaluated using the velocity at the input points. This forced response can be computed using any suitable finite element dynamic solver. It's noteworthy that strain energy densities and velocities are typically standard outputs provided by most finite element solvers. The dissipated power density is to be computed according to the dissipation models. Since there are many ways to model dissipation in finite element modeling, the dissipated power density computation may appear not as straightforward as one would expect. In any case, the overall energy balance of the system can be easily checked by comparing the total injected power with the total dissipated power. In this paper, only localized viscous damping and global proportional (to stiffness) structural damping are considered.

Secondly, the diffusion equation Eq. (11) is solved using a thermal solver applied to the same finite element geometry, with a uniform unitary thermal conductivity. As mentioned in the previous paragraph, non-dissipative mechanical connections have to be changed into linear relations ensuring the vibrational temperature continuity. Injected and dissipated power density are incorporated as thermal loads all over the structure. Fig. 2 illustrates the flowchart of the irrotational intensity calculation.

In practice, all results presented in this paper are computed using Nastran. The dynamic response is obtained from a modal frequency response analysis (SOL111), and the thermal response corresponds to a steady-state thermal analysis (SOL 153). Whatever the dynamic solver that is used, its necessary consistency ensures the whole system's energy balance. As previously mentioned, the condition of equal vibrational temperature across non-dissipative connections is achieved using MPCs in Nastran. Since the method relies on finite element modeling, any kind of elementary modeling can be addressed as soon as these elements are supported for both dynamic and thermal solutions: solids, shells, and beams. In the case where some mechanical modeling would not be supported in the thermal solver, the thermal model would have to be adjusted by substituting appropriate elements, with the same geometry. Any software providing both dynamic and thermal solvers could be used to apply the proposed methodology. Depending on the software capabilities, few external operations may be required, referred to as in-house programs on Fig. 2. The thermal solver's fi-

nal output being a temperature field, a general purpose finite element post-processing software is required to complete the analysis and get the irrotational intensity (temperature gradient), streamlines or compute power flows through selected contours. Depending on the finite element software capabilities, the intensity field as well as power flows on contours could be natively computed saving post-processing operations. Results presented in this paper are processed and plotted in META.

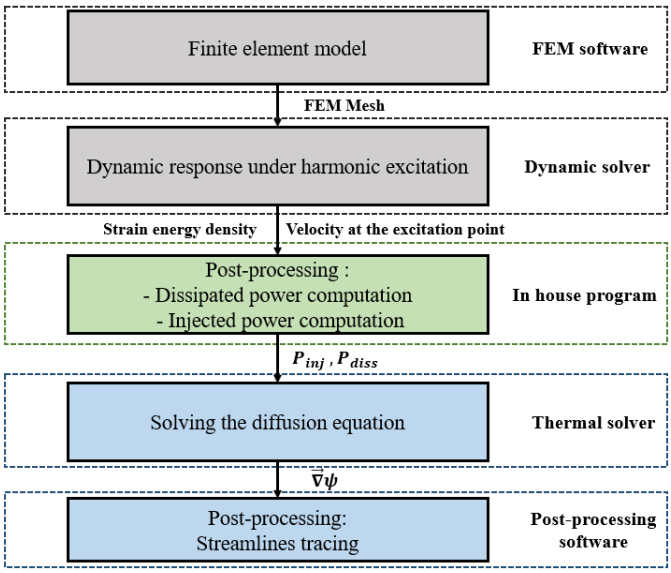

Fig. 2. Scheme of the computational system for the irrotational intensity field

ASSESSMENT OF THE IRROTATIONAL INTENSITY COMPUTATION IN A PLATES ASSEMBLY

The methodology is first checked on a simple plates assembly interconnected through point connections (spot welds), as illustrated in Fig. 3. Plates are numbered 1 to 7. The load is applied on plate 1. All plates are modeled using PSHELL elements and spot welds are modeled by non-dissipative CBUSH/CBAR elements, as shown in Fig. 4. Plate meshes are incompatible as one would expect for an industrial structure model. All plates have uniform properties that are shown in Tab.1.

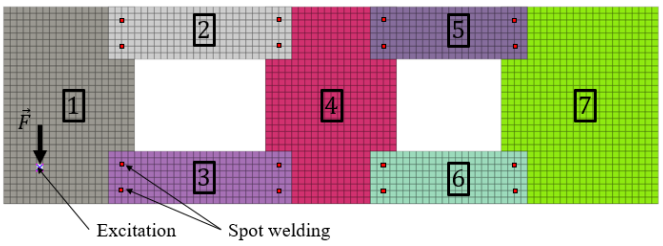

Fig. 3. Finite element model of assembled plates

The structure is loaded by a harmonic force of $1\,\mathrm{N}$, normal to the surface. The force is applied via an RBE2 element, in order to avoid the singularities that may arise when applying the force to a single node. The dissipation is

Thickness (mm)	1
Elastic modulus (MPa)	210 000
Poisson ratio	0.3
Bulk density (kg/m^3)	7 800
Structural damping	1%

Table 1: Plate properties

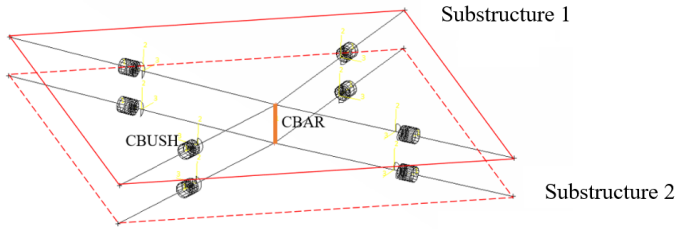

Fig. 4. Finite element model of welding points

modeled by structural proportional damping (PARAMG). The numerical resolution (NASTRAN SOl111) includes the calculation of residuals (RESVEC) to ensure a better convergence of the solution. The velocity response for a frequency of 1000 Hz is plotted in Fig. 5. Considering the plate's size and thickness, this frequency is high enough to fulfill the mid-frequency domain assumptions: no global mode of the assembled structure can be seen. Although some local modal behavior appears, a global decrease in the response can be observed away from the source.

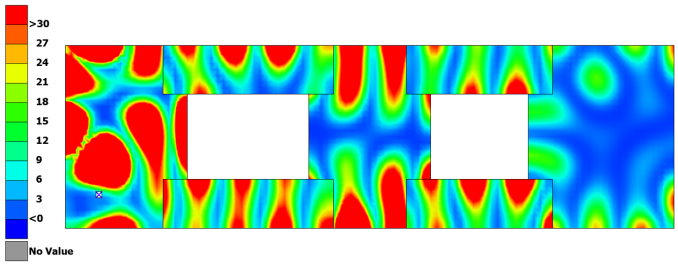

Fig. 5. Dynamic velocity Response $(\mathbf{v}^2\ (\mathrm{mm\,s^{-1}})^2)$ at $1000\,\mathrm{Hz}$

As mentioned above, in-house processing is then used to set up the associated thermal problem to be able to derive the irrotational intensity. Fig. 6 shows the result of the thermal solution (NASTRAN SOL153) e.g. the vibrational temperature. As it could be expected, the vibrational temperature appears very smooth. Away from plate 1, the temperature is decreasing and seems consistent with the dynamic response. Nevertheless, these figures show that the relationship between the vibrational temperature and the dynamic response is not straightforward, and requiring further developments.

The smooth temperature field suggests some stability regarding frequency. Since this stability would be related to the strain energy field -still heterogeneous in the mid-frequency range-, some investigations are required before

allowing a drastic reduction of the number of frequency points.

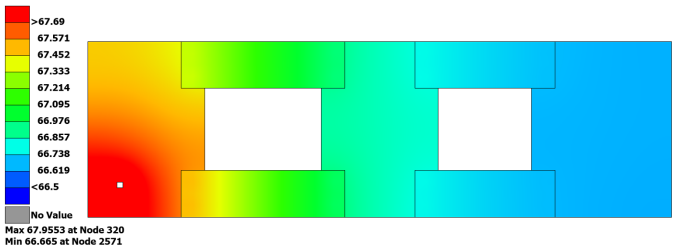

Fig. 6. Vibrational temperature ψ (in W) at $1000\,\mathrm{Hz}$.

INTENSITY FIELD ANALYSIS

Fig. 7 presents the structural intensity field distribution at $1000\,\mathrm{Hz}$. This field is obtained by applying the structural intensity expression (2), using the corresponding functionality available in META. The vector field is represented here by fixed length arrows colored by the vector norm. Although the expected global trend of a field decreases from plate 1 to plate 7, the transmission path appears fuzzy because of many vortices. Transmission from plate 1 to plate 4 seems to occur mostly through plate 2. From plate 4 to plate 7, the dominant path seems to be through plate 6.

Fig. 8 shows the irrotational intensity field at $1000\,\mathrm{Hz}$ computed by the proposed hybrid approach. The resulting field appears much smoother and easily readable. No more vortices can be seen and the scheme is consistent with our knowledge of vibration propagation. The transmission path clearly shows a dominating path to plate 4 through plates 3 that is aligned with the excitation point on plate 1. Transmission from plate 4 to plate 7 appears balanced between plates 5 and 6.

This first example highlights how much a qualitative interpretation of the total intensity field is misleading.

At this point, it can also be noticed that the transmission path that appears to be influenced by the source location could not be grasped by the SEA model that, by construction, would assume a homogeneous rain-on-roof excitation.

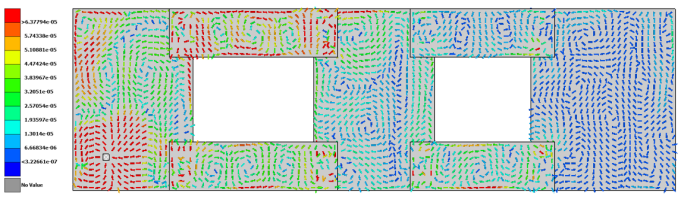

Fig. 7. Structural intensity field at $1000\,\mathrm{Hz}$

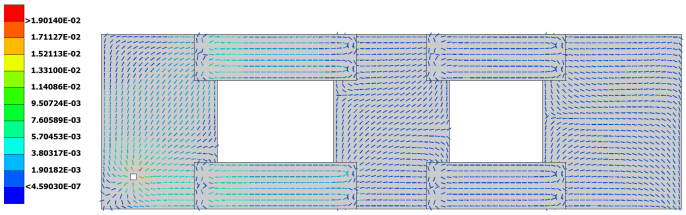

Fig. 8. Irrotational intensity field at $1000\,\mathrm{Hz}$

POWER BALANCE

Apart from a qualitative analysis of the transmission paths, it may be useful and more objective to consider the power flows between the different plates. Power flow computations also allow checking the model consistency e.g. the global and local power balances.

Table 2 shows the power dissipated in each of the plates. The injected power, $P_{inj} = 0.49$, appears to be the exact sum of the dissipated powers ensuring the model consistency. One could notice here that the power dissipated in plate 2 is much larger than for plate 3. Consistently, Fig. 5 indicates a higher response for plate 2 leading to a higher dissipated power than in plate 3. One can also notice that the power dissipated in plate 7 is the same as plate 3, although its vibrational level appears smaller in the Fig. 5. That is due to the larger size of plate 7.

P_{diss1}	P_{diss2}	P_{diss3}	P_{diss4}	P_{diss5}	P_{diss6}	P_{diss7}
0.15	0.12	0.04	0.09	0.03	0.03	0.04

Table 2: Power dissipated by each plate at $1000\,\mathrm{Hz}$. P_{dissi} is the power dissipated by the plate i

Table 3 shows the powers exchanged between the plates at $1000\,\mathrm{Hz}$ respectively computed from the total structural intensity, irrotational intensities and rotational intensities. Comparing table 3 and table 2 show that for both the total structural intensity and the irrotational intensity the local balance is achieved such that $P_{dissj} = \sum_i P_{ir,i\to j}$. As already mentioned above, the rotational intensity does not contribute to the power balance since $\sum_i P_{r,i\to j} = 0$.

As it was already observed in ([11]) for the case of a one-piece mesh, the rotational intensity skews the power flow computations. In this application, this is especially obvious in the analysis of the power input to plate 7: while the irrotational intensity shows the equivalent contribution from plates 5 and 6 -which makes sense-, the power flow computed from the total intensity is biased, showing a reverse flow to plate 5. It can also be noticed that despite a higher dynamic response, the power flow from plate 2 to plate 4 remains lower than the one from plate 3 to plate 4. Finally, the power flow from plate 4 to plate 7 is balanced between plate 5 to plate 6, as it would be predicted from an SEA model.

This academic application illustrates how the proposed

methodology provides an accurate analysis of power flows at a system level. This information could certainly be advantageously used to improve the SEA analysis that is obviously refuted here.

Interface	Total	Irrotationnal	Rotationnal
$P_{1\to2}$	0.16	0.18	-0.02
$P_{1\to3}$	0.18	0.16	0.02
$P_{2\to4}$	0.04	0.06	-0.02
$P_{3\to4}$	0.14	0.12	0.02
$P_{4\to5}$	0.02	0.04	-0.03
$P_{4\to6}$	0.08	0.05	0.03
$P_{5\to7}$	-0.01	0.02	-0.03
$P_{6\to7}$	0.05	0.02	0.03

Table 3: Power exchanged between plates at $1000\,\mathrm{Hz}$. $P_{i\to j}$ the power exchanged between the plates i and j.

APPLICATION TO AN INDUSTRIAL STRUCTURE

The application of the irrotational intensity computation in an industrial context begins with an analysis of a front longitudinal rail.

Fig. 9 shows the finite element model of the right front longitudinal rail, which is made up of three stamped parts assembled by spot welds. The finite element model consists of quadrangular and triangular elements. The spot welds are modeled by CBUSH-CBAR-CBUSH non-dissipative elements. Dissipation is modeled by a modal structural damping of 1%. A harmonic unit force is applied to a rigid RBE2 element in the y direction. Such a component behaves as a beam at low frequencies while it tends to behave as a shell for higher frequencies.

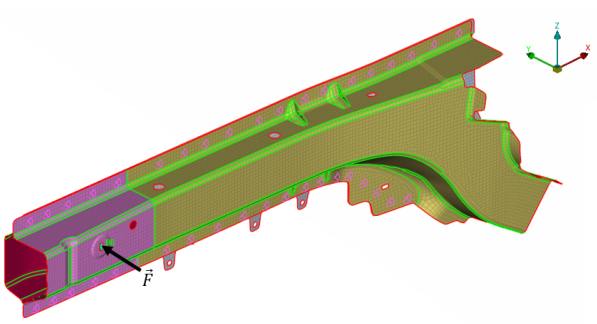

Fig. 9. Finite element model of a right front longitudinal rail

IRROTATIONAL INTENSITY FIELD DISTRIBUTIONS

Fig. 10 shows the irrotational intensity field in the side rail for three different frequencies: $1000\,\mathrm{Hz}$, $2000\,\mathrm{Hz}$ and $2500\,\mathrm{Hz}$. The irrotational intensity is represented by fixed length arrows at the mesh scale which makes it difficult to read. Nevertheless, it can be perceived that it is smoothly organized along the rail, regardless of the geometry and the frequency. Arrows are colored by the vibrational temperature highlighting the gradient, which also appears to be smooth. These similar patterns for the different frequencies are governed by the same dissipation scheme (uniform structural damping). This representation is in line with an intuitive one-dimensional vibrational energy propagation scheme. Indeed, for a beam-like component, except in the vicinity of the loading point, one might expect a uniform distribution perpendicular to the neutral axis of the beam.

Close to the loading point, one can observe a zone where local behavior predominates over the global beam behavior. It is in this zone that reinforcement should be applied to fully take advantage of the beam's stiffness. It's noteworthy that, unlike previous configurations, in this representation of the intensity field, we have not normalized the values with respect to the injected power. For this reason, no conclusion will be drawn about the extend of this local behavior.

The presentation of the irrotational intensity field in this industrial case study serves a dual purpose: firstly, it demonstrates the practical application of our methodology to real industrial structures, and secondly, it emphasizes the ease of analysis allowed by the irrotational intensity, despite the structural complexity.

CONCLUSION

In this paper, a new methodology, based on the irrotational intensity computation for a standard finite element model, was extended to the case of assembled structures such as car bodies. The irrotational intensity is computed by cascading a dynamic response and a thermal response applied to -mostly- the same finite element model. Mechanical connections between the structural components are transformed into vibrational temperature continuity equations, expressed as linear relationships between nodal thermal unknowns. The consistency of the approach was checked in the case of a simple assembly of rectangular flat plates. The results analysis highlights the relevance of the irrotational intensity both from qualitative (transfer path) and quantitative (power flows) points of view.

The method is finally applied to a real body-in-white component, with some geometrical and mechanical complexity. Again the method proves its ability to provide a straightforward understanding of vibration propagation at mid and high frequencies. Work is in progress for an automatic conversion into thermal connection of the thousands of mechanical connections that take part in a full BIW assembly.

Further work is still required to clearly establish the relationship between the vibrational temperature and the dynamic response as well as the connections that could be made with SEA. In particular, it is expected that avoiding the statistics over the loads (rain-on-the-roof excitation of SEA) and a better estimation of power flows (using irrotational intensity) and dissipated power (related to strain

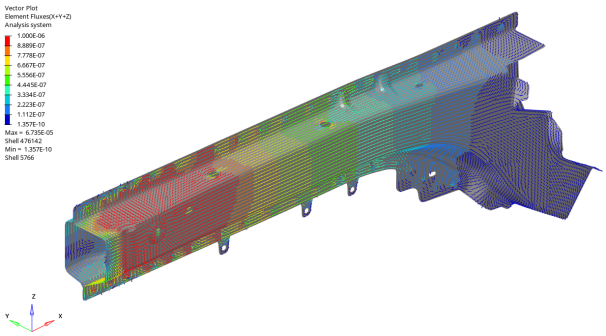

(a) 1000 Hz

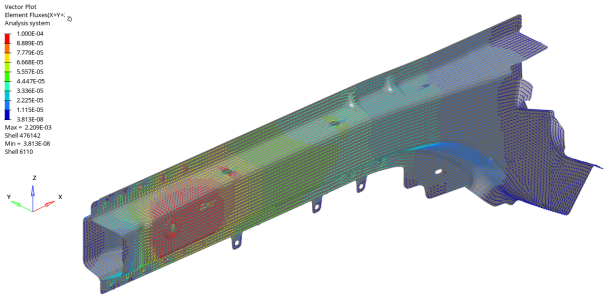

(b) 2000 Hz

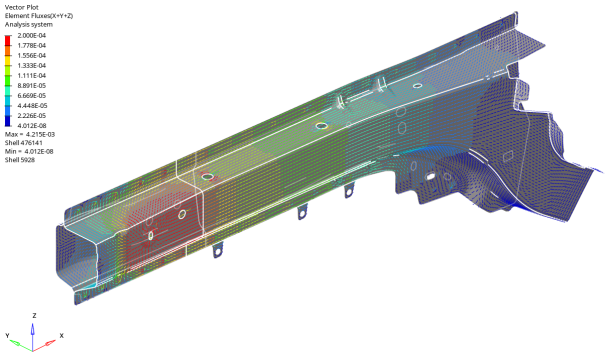

(c) 2500 Hz

Fig. 10. Irrotationnal intensity in a right front side rail.

energy instead of kinetic energy) would help to improve SEA models that remain an efficient sensitivity tool at the system level.

REFERENCES

[1] G. Pavić. Measurement of structure borne wave intensity, part i: Formulation of the methods. *Journal of Sound and Vibration*, 49(2):221–230, 1976.

[2] L. Gavric and G. Pavic. A finite element method for computation of structural intensity by the normal mode approach. *Journal of Sound and Vibration*, 164:29–43, 1993.

[3] J. C. Pascal. Expressions simplifiées du flux d'énergie dans les plaques. *Le Journal de Physique IV*, 2(C1):C1–515, 1992.

[4] R. H. Lyon and G. Maidanik. Power flow between linearly coupled oscillators. *The journal of the Acoustical Society of America*, 34(5):623–639, 1962.

[5] G. Maidanik. Response of coupled dynamic systems. *Journal of Sound and Vibration*, 46(1):561–583, 1976.

[6] F. J. Fahy. Statistical energy analysis: a critical overview. *Philosophical Transactions of the Royal Society of London. Series A: Physical and Engineering Sciences*, 346(1681):431–447, 1994.

[7] O. M. Bouthier and R. J. Bernhard. Simple models of the energetics of transversely vibrating plates. *Journal of Sound and Vibration*, 182:149–164, 1995.

[8] R. S. Langley. On the vibrational conductivity approach to high frequency dynamics for two-dimensional structural components. *Journal of Sound and Vibration*, 182:637–657, 1995.

[9] L. Gagliardini, L. Houillon, G. Borello, and L. Petrinelli. Virtual sea-fea-based modeling of mid-frequency structure-borne noise. *Sound and vibration*, 39(1):22, 2005.

[10] A. Wang and N. Vlahopoulos. Vehicle nvh analysis using efea & ebea methods. *SAE International Journal of Passenger Cars-Mechanical Systems*, 2(2009-01-0766):814–821, 2009.

[11] J. Takhchi, M. Ouisse, E. Sadoulet-Reboul, N. Bouhaddi, L. Gagliardini, F. Bornet, L. Gavric, and F. Lakrad. A method to investigate mid and high-frequency vibration energy transfer paths using the irrotational intensity. *Journal of Sound and Vibration*, 572, 2024.

[12] G. Pavic. The role of damping on energy and power in vibrating systems. *Journal of Sound and Vibration*, 281:45–71, 2005.

[13] W. V. D. Hodge. *The theory and applications of harmonic integrals*. Cambridge University Press archive, 1989.

CONTACT INFORMATION

laurent.gagliardini@aitl.fr

frederic.bornet1@stellantis.com